Electro-Optical Nanotraps for Neutral Atoms

Brian Murphy[1] and Lene Vestergaard Hau[1,2]

[1]School of Engineering and Applied Sciences, Harvard University, Cambridge, Massachusetts 02138, USA
[2]Department of Physics, Harvard University, Cambridge, Massachusetts 02138, USA

(Received 26 August 2008; published 22 January 2009)

We propose a new class of nanoscale electro-optical traps for neutral atoms. A prototype is the toroidal trap created by a suspended, charged carbon nanotube decorated with a silver nanosphere dimer. An illuminating laser field, blue detuned from an atomic resonance frequency, is strongly focused by plasmons induced in the dimer and generates both a repulsive potential barrier near the nanostructure surface and a large viscous damping force that facilitates trap loading. Atoms with velocities of several meters per second may be loaded directly into the trap via spontaneous emission of just two photons.

DOI: 10.1103/PhysRevLett.102.033003 PACS numbers: 37.10.Gh, 37.10.De, 73.22.Lp, 78.67.Bf

Laser cooling and trapping of neutral atoms have led to remarkable successes including the creation of Bose-Einstein condensates [1], and a quest to miniaturize and chip-integrate trapping and cooling structures has represented an extremely active research area in recent years [2]. Cold atoms have successfully been trapped in micron-sized traps, but efforts to push the technology to the nanoscale have been unsuccessful. Proposals for atomic traps near nanostructures have been put forward [3]; however, methods to overcome the attractive van der Waals forces near material surfaces [4] as well as the heating caused by thermally induced charge and current fluctuations in room temperature materials in close proximity to trapped atoms [5] have not yet been proposed. Here we present an electro-optical nanotrap that overcomes these obstacles and, importantly, also provides for damping of atomic motion that facilitates direct trap loading.

The strong coupling of a trapped atom to the nanoscopic structure allows for sensitive probing of electromagnetic fields and dielectric properties of materials at the nanoscale, of great importance for the flourishing field of single biomolecule studies with surface enhanced Raman scattering [6]. It also facilitates studies of QED effects in atom-surface interactions, a topic of intense current interest for applications to nanomechanical devices and in the search for forces beyond the standard model [7].

Metallic nanoparticles exhibit plasmon resonances. An illuminating electromagnetic field can excite plasma oscillations that generate large and localized electric fields near the particles [6]. Here, we consider the effect of such fields on atomic motion. A plasmon-resonant laser field that is blue detuned from an atomic resonance causes a dramatic repulsion of atoms from the nanostructure surface, and when combined with attractive electrostatic forces creates a trap minimum at nanometer distances from that surface. Simultaneously, large gradients of the plasmon-enhanced fields provide a strong dissipative force.

As diagrammed in Fig. 1, a nanotrap is formed by two Ag spheres that are supported and charged by a carbon nanotube. Suspended nanotubes with lengths of many microns have been fabricated across gaps [8].

As described in detail below, the trapping potential for an atom near the nanospheres is approximated by

$$U_{\text{trap}} = U_L + U_g + V_g, \tag{1}$$

where U_g is the dc Stark shift and V_g the van der Waals energy of the ground state. Also, $U_L = \frac{\hbar\delta}{2}\ln(1+s)$ is the optical dipole potential [9,10] due to the plasmon-enhanced laser field, where $s = \frac{\Omega^2/2}{\gamma^2/4+\delta^2}$ is the saturation parameter, δ is the detuning between the laser and the atomic resonance including dc Stark shifts and van der Waals shifts, γ is the decay rate of the excited atomic state modified by the presence of the nanostructure as discussed later in the text, and $\Omega = \frac{\mu E_0^L}{\hbar}$ is the Rabi frequency repre-

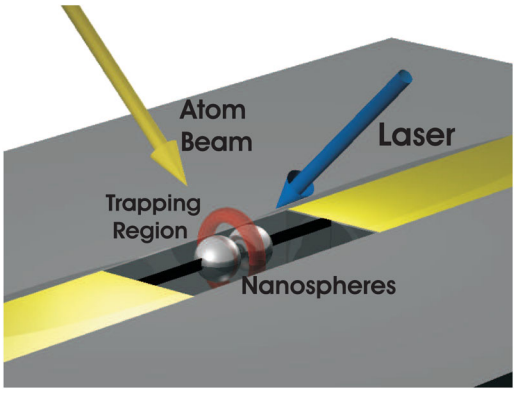

FIG. 1 (color online). The nanotrap. A suspended carbon nanotube, attached at each end to an electrode, supports two Ag nanospheres across a gap in a silicon nitride membrane. An illuminating laser field excites plasma oscillations in the spheres, and large electric fields near the structures are generated. In addition, a dc voltage is applied to the electrodes to create a toroidal trapping region (red). The radius of the toroid can be controlled with nanometer precision and the trap may be loaded directly from an incident atom beam.

senting the coupling of the plasmon-enhanced electric field of amplitude E_0^L to the atomic dipole moment μ.

To solve for both the static and laser-induced electric fields in the near field, we work in the quasistatic limit. For an incident plane wave laser field $\mathbf{E}^{\text{inc}}$ at frequency ω, the resulting electric field is $E_j^L(\mathbf{r}) = M_{ji}(\mathbf{r}, \omega)E_i^{\text{inc}}$, where M describes the local, plasmon-induced enhancement. For an external dipole source $\mathbf{p}$ oscillating at frequency ω at location $\mathbf{r}'$, the induced charge distribution in the nanostructure creates a reflected electric field $E_j^{\text{ref}}(\mathbf{r}) = G_{ji}(\mathbf{r}, \mathbf{r}'; \omega)p_i$, where G is the tensor Green's function for the given geometry. The dc electric field $\mathbf{E}^{\text{dc}}$ is calculated with the spheres fixed at a particular voltage, and in all three cases we use the dielectric constant ε_{Ag} of Ag at the relevant source frequency [11]. Figure 2 shows the resulting trapping potential (1) for an atom with unit oscillator strength and a resonance frequency close to the plasmon resonance of the dimer-tube structure.

The illuminating laser will cause heating in the nanospheres at a rate of 2 μW per sphere, resulting in a dimer temperature of ≈ 640 K which is well below the melting point of silver. Here we assume a 10 μm long, 4 nm diameter nanotube fixed to a 300 K membrane [12].

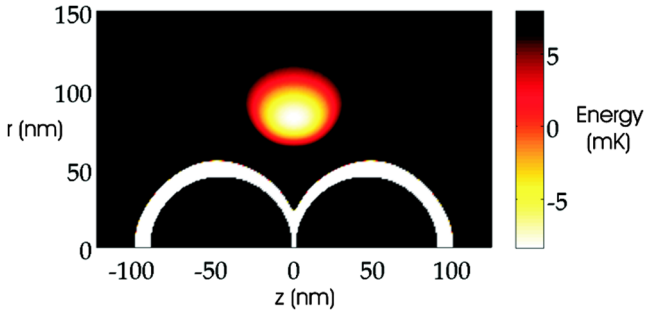

FIG. 2 (color online). The trap potential (1). The z axis is parallel to the nanotube, and r is the distance from the tube. Incident laser light of wavelength $\lambda = 475$ nm is polarized along the z axis connecting two Ag spheres of diameter 90 nm and separation 2 nm. The plasmon resonance of this dimer is at 457 nm. The detuning between the laser frequency ω and the bare atomic resonance ω_0 is picked to be $\Delta = \omega - \omega_0 = 500\Gamma$, where $\Gamma = q^2\omega_0^2/6\pi\varepsilon_0 m_e c^3$ is the decay rate of the excited atomic state in free space. The incident laser intensity is $I^{\text{inc}} = 4.6 \times 10^3$ W/cm^2, and the nanospheres are charged to a voltage of $V = 3.5$ V (relative to a macroscopic grounding surface). With these parameters, the saturation parameter $s = 0.09$ at the trap minimum. For contrast, the color scale has a lower limit corresponding to the minimum value of U_{trap} in the trapping region and a range equal to the equilibrium temperature. The low energy area near the surface of the nanospheres is the region where the attractive van der Waals force dominates, and is not part of the trapping region. The trapping potential has cylindrical symmetry in the quasistatic limit. When the voltage is turned off, a trapping potential persists due to a minimum in the laser field amplitude at $r = 94$ nm, but the barrier for escape is reduced in this case from 48 to 29 mK.

We model an atom's internal structure with a single ground state $|g\rangle$ and three excited states $|e_r\rangle$, $|e_\phi\rangle$, and $|e_z\rangle$ that are degenerate for a free-space atom. The dipole matrix element is $\langle e_i|\hat{\mathbf{d}}|g\rangle = \mu\hat{i}$, where $\{\hat{i}\}_{i=r,\phi,z}$ form orthonormal basis vectors in a cylindrical coordinate system, $\mu = \sqrt{\hbar q^2/2m_e\omega_0}$ (the value for a two-level atom), q is the electron charge, m_e is the mass of the electron, and ω_0 is the resonance frequency of the atom. The plasmon-enhanced electric field of the laser is $\mathbf{E}^L = \frac{1}{2}E_0^L\hat{\boldsymbol{\epsilon}}e^{-i\omega t} +$ c.c., where E_0^L and $\hat{\boldsymbol{\epsilon}}$ are the position-dependent amplitude and polarization vector. We change two of the excited state basis vectors to $|e\rangle = \epsilon_r|e_r\rangle + \epsilon_z|e_z\rangle$ and $|e_\perp\rangle = \epsilon_z^*|e_r\rangle - \epsilon_r^*|e_z\rangle$. The Hamiltonian (in the rotating frame) governing the internal dynamics of an atom interacting with the charged and laser-illuminated nanotube-dimer system is then

$$\hat{H} = (V_g + U_g)|g\rangle\langle g| + (-\hbar\Delta + V_e + U_e)|e\rangle\langle e| - \frac{\hbar\Omega}{2}(|e\rangle\langle g| + |g\rangle\langle e|). \tag{2}$$

Here V_e and U_e are the van der Waals and dc Stark shifts of the excited state $|e\rangle$, and we have used the rotating wave approximation and the fact that the laser couples only states $|g\rangle$ and $|e\rangle$ to an excellent approximation. From (2), we find the force on an atom at rest to be

$$\langle\mathbf{F}\rangle = -\frac{\hbar\delta\Omega\nabla\Omega}{2(1+s)(\gamma^2/4+\delta^2)} + \frac{\hbar s\nabla\delta}{2(1+s)} - \nabla(V_g + U_g), \tag{3}$$

where $\delta = \Delta - (V_e + U_e - V_g - U_g)/\hbar$ and $\Delta = \omega - \omega_0$. In the regime of large and relatively constant detuning ($\delta \gg \gamma$ and $|\frac{\nabla\delta}{\delta}| \ll \frac{|\nabla\Omega|}{\Omega}$), the force in (3) is minus the gradient of the trap potential in (1) which is plotted in Fig. 2.

The dc Stark shifts of the ground and excited states are $U_g = -\frac{1}{2}\alpha_0|\mathbf{E}^{\text{dc}}|^2$ and $U_e = \frac{1}{2}\alpha_0|\mathbf{E}^{\text{dc}}\cdot\hat{\boldsymbol{\epsilon}}|^2$, where the static polarizability is given by $\alpha_0 = \frac{q^2}{m_e\omega_0^2}$. (Since $\Delta \gg U_e/\hbar$ and $s \ll 1$ in the trap region for the parameters used here, the atom dynamics do not depend on the specific form of U_e.)

For a nanoscale trap, van der Waals (and Casimir-Polder [13]) shifts and modifications to the excited state lifetime are important. In the near field, the ground state energy shift of an atom in front of a perfect, planar conductor is the London energy of a fluctuating dipole moment interacting with its image dipole. Here we approximate the van der Waals shift of the ground state by the energy of a fluctuating dipole in front of two conducting spheres, $V_g \approx -\frac{1}{2}|\mu|^2\sum_{i=r,\phi,z}G_{ii}^{\text{stat}}$, where $G_{ii}^{\text{stat}} = G_{ii}(\mathbf{r}, \mathbf{r}; \omega = 0)$.

Excited state van der Waals shifts have two contributions, of which one is an inverted ground state van der Waals shift and the other is due to a modification of the resonance frequency of a Lorentz oscillator from the

oscillator's self-interaction with the induced, reflected field from the nanostructure [14]. Hence $V_e \approx \frac{1}{2}|\mu|^2 \sum_{i=r,z} |\epsilon_i|^2 (G_{ii}^{\mathrm{stat}} - 2\,\mathrm{Re}(G_{ii}^{\mathrm{res}}))$, where $G_{ii}^{\mathrm{res}} = G_{ii}(\mathbf{r}, \mathbf{r}; \omega_0)$ [15].

The decay rate of the excited state is also modified [16] due to the proximity of the atom to the nanostructure. The decay rate calculated from the damping of a classical, oscillating dipole interacting with its induced electric field from the nanostructure agrees with a full quantum treatment [14]. In the quasistatic limit, this damping yields only the nonradiative decay rate corresponding to energy loss in the nanostructure [17] according to

$$\frac{\gamma_{nr}}{\Gamma} = \frac{6\pi\varepsilon_0}{k^3} \sum_{i,j=r,z} \mathrm{Im}(\epsilon_i \epsilon_j^* G_{ji}^{\mathrm{res}}), \tag{4}$$

where Γ is the free-space decay rate. The radiative decay γ_r can then be added separately. From energy conservation, we find γ_r by calculating the energy radiated into the far field. We can relate the dipole far field emission to the local field enhancement of an incident plane wave by appealing to the reciprocity theorem [18] and find

$$\frac{\gamma_r}{\Gamma} = \sum_{i,j,k=r,z} \epsilon_i \epsilon_j^* M_{ik} M_{jk}^*. \tag{5}$$

We then obtain $\gamma = \gamma_r + \gamma_{nr}$ everywhere in space from (4) and (5).

For an atom to be stably trapped, the equilibrium temperature characterizing the average kinetic energy of its center-of-mass motion must be less than the potential barrier for trap escape. A strong blue-detuned laser field leads not only to trapping (3) but also to damping [10]. In the "strong-field limit" where $\Omega, \delta, s\Omega, s\delta \gg \gamma$, and to first order in velocity, the damping of the center-of-mass motion is given by the force

$$\mathbf{F} \approx -\frac{\hbar s^2}{\delta\gamma(1+s)^3}((\nabla\Omega)\cdot\mathbf{v})\nabla\Omega. \tag{6}$$

Its dependence on the gradient of the Rabi frequency leads to extraordinarily large damping rates with the strongly localized fields of the nanotube-dimer trap. (The linear velocity dependence of the damping force is valid for velocities below a critical velocity $v_c \approx \gamma\Omega/|\nabla\Omega|$.) Furthermore, an atom is heated due to fluctuations of the trapping force from spontaneous transitions associated with the damping. The heating is characterized by a momentum diffusion coefficient D, and in the strong-field limit, $D \approx \frac{\hbar^2 s^3}{2\gamma(1+s)^3}|\nabla\Omega|^2$ [10]. The equilibrium temperature for atomic motion is given by the ratio between D and the damping (velocity) coefficient of (6), averaged over an isotropic velocity distribution, so $k_B T = \frac{\hbar\Omega^2}{4\delta}$. With the parameters of Fig. 2, this would lead to an equilibrium temperature of 16 mK which is below the potential barrier of 48 mK for trap escape.

Atoms are trapped with a transverse oscillation period of 50 ns. This is on the order of the inverse spontaneous decay rate γ, which leads us to reexamine the microscopic nature of the damping mechanism. We perform Monte Carlo simulations of atom trajectories, and for motion along the $z = 0$ symmetry axis we show in Fig. 3 how an atom spontaneously transitions between the energy curves corresponding to the two "dressed" eigenstates, $|1\rangle$ and $|2\rangle$, of the Hamiltonian (2) [10]. (In our case, the eigenstates are "dressed" by plasmons and are determined by the coupling between the atom and the longitudinal, plasmon-induced electric field.) We find that the time τ an atom remains trapped in dressed state $|1\rangle$ increases when the voltage is turned off and can be tuned over many orders of magnitude. We find $\tau = 25\ \mu$s for $\Delta = 500\Gamma$, whereas

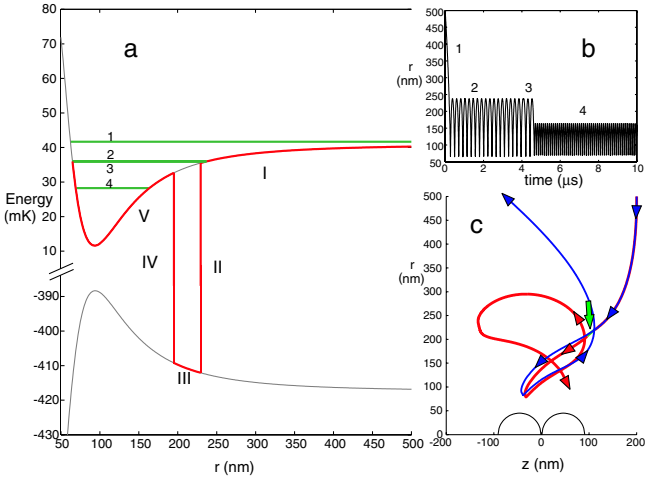

FIG. 3 (color online). Atom trajectories studied with Monte Carlo simulations. In (a) we show a typical capture process for an atom launched along the $z = 0$ symmetry axis with velocity 1 m/s at $r = 500$ nm (corresponding to a launch velocity of 5.5 m/s from infinity). The dressed state energies are plotted as gray curves (top curve is for $|1\rangle$ and bottom curve for $|2\rangle$), and the state actually occupied by the atom is marked in red (and labeled I, III, V). [In the limit of vanishing laser field $|1\rangle$ ($|2\rangle$) is simply $|g\rangle$ ($|e\rangle$) but for nonzero field, the dressed states are superpositions of $|g\rangle$ and $|e\rangle$ [10].] In regions I and V the atom is in dressed state $|1\rangle$, in region III it is in state $|2\rangle$, and after transitions II and IV the particle has suffered a net energy loss. The energy dissipation in such processes is provided by loss in the nanoparticle and by emission of fluorescence photons with frequencies upshifted or downshifted relative to the laser frequency by amounts given by the energy differences between the dressed states. In (b) the same atomic motion is followed further, for up to 10 μs. The successive stages, corresponding to different energies reached after each pair of transitions, are labeled 1–4 in both (a) and (b). In (c), Monte Carlo trajectories are plotted for both uncaptured (blue) and captured (red) atoms launched with velocity 1 m/s from $(r, z) = (500, 200)$ nm. [The paths are followed for 734 ns and 1.1 μs, respectively.] The captured atom undergoes a pair of spontaneous transitions in the region indicated by a separate arrow (green).

$\Delta = 6000\Gamma$ results in $\tau = 900$ ms. Heating due to Johnson noise in the nanospheres is negligible on this time scale. This is very different than for magnetic microtraps where large amounts of conducting material are in close proximity to trapped atoms [5].

Monte Carlo simulations have also been used to study the loading of atoms into the nanotrap. We find that an atom launched towards the nanostructure with a velocity of meters per second may lose enough energy to become trapped after a single pair of spontaneous transitions between the dressed states. Figure 3(a) shows how an incoming atom in state $|1\rangle$ transitions to $|2\rangle$ and then loses kinetic energy as it climbs ''uphill'' in this state. After the reciprocal transition $|2\rangle \rightarrow |1\rangle$, the atom remains trapped in $|1\rangle$, having lost potential and kinetic energy in equal amounts. The energy is dissipated via the atom's coupling to plasmon oscillations that are subsequently damped both by coupling to the transverse (radiating) electromagnetic field modes and by loss in the nanostructure. In Fig. 3(b) we continue to follow the motion of the trapped atom for 10 μs. These simulations do not rely on Eqs. (3) and (6).

The nanotrap can be loaded by atoms launched at a few meters per second from a high-density magneto-optical trap. We estimate that with nanotrap parameters as in Fig. 2 (except with a nanotube voltage of $V = 0$), a magneto-optical trap density of 10^{12} cm^{-3}, a launch velocity of 5.5 m/s, and a longitudinal temperature of 200 μK [19], there is an approximately 2% probability for atom capture within a cross-sectional area of 450 nm (Δz) by 800 nm [Fig. 3(c)]. This results in an average loading time of 25 μs, and after a brief loading stage, the laser detuning may be increased to maximize the trap lifetime. To match the plasmon resonance with a particular atomic resonance, the nanotube may be decorated with dimers of nanoshells rather than solid silver spheres [20]. Surface adsorption of atoms is prevented with heated silver spheres as used here (and for sodium atoms, by an ionization potential that is much larger than the work function for silver) [21].

We have described a novel nanotrap for neutral atoms. The trap frequency is several MHz, the ground state is transversely localized to within a few nm, and trap lifetimes exceed 10^6 oscillation periods. Atoms can be held in multiple hyperfine states facilitating sideband cooling to the ground state [22]. Spectroscopic determination of the trap's energy levels, with parts-per-million precision, is possible with rf fields applied directly to the nanotube. The trap minimum is in the crossover region between the Casimir-Polder and the van der Waals–London regimes [7], and in the limit of large laser detuning, nanotrap studies could cast new light on the interplay between quantum fluctuations in the radiation field, the atom, and the nanostructure [23], with a proper description ultimately involving entangled eigenstates of the strongly coupled atom-nanostructure system. Atom-surface interactions have recently been a subject of intense studies that have opened new possibilities for testing the existence of non-Newtonian gravitational forces at small length scales [24]. Studies based on the nanotrap have the potential to push such tests to length scales of 100 nm and below, a regime inaccessible in prior experiments.

This work was supported by the Air Force Office of Sponsored Research.

[1] E. A. Cornell and C. E. Wieman, Rev. Mod. Phys. **74**, 875 (2002); W. Ketterle, Rev. Mod. Phys. **74**, 1131 (2002).
[2] J. Fortagh and C. Zimmermann, Rev. Mod. Phys. **79**, 235 (2007).
[3] V. I. Balykin, V. V. Klimov, and V. S. Letokhov, JETP Lett. **78**, 8 (2003); J. P. Burke *et al.*, Phys. Rev. A **65**, 043411 (2002).
[4] R. Fermani, S. Scheel, and P. L. Knight, Phys. Rev. A **75**, 062905 (2007).
[5] C. Henkel, S. Pötting, and M. Wilkens, Appl. Phys. B **69**, 379 (1999); M. P. A. Jones *et al.*, Phys. Rev. Lett. **91**, 080401 (2003); D. Harber, J. McGuirk, J. Obrecht, and E. Cornell, J. Low Temp. Phys. **133**, 229 (2003); P. Rekdal, S. Scheel, P. Knight, and E. A. Hinds, Phys. Rev. A **70**, 013811 (2004).
[6] J. Jiang *et al.*, J. Phys. Chem. B **107**, 9964 (2003).
[7] M. Antezza, L. P. Pitaevskii, and S. Stringari, Phys. Rev. A **70**, 053619 (2004), and references therein.
[8] H. B. Peng *et al.*, Appl. Phys. Lett. **83**, 4238 (2003); L. Huang *et al.*, J. Phys. Chem. B **110**, 11 103 (2006).
[9] A. Ashkin, Phys. Rev. Lett. **40**, 729 (1978).
[10] J. Dalibard and C. Cohen-Tannoudji, J. Opt. Soc. Am. B **2**, 1707 (1985).
[11] *Handbook of Optical Constants of Solids*, edited by E. D. Palik (Academic, Orlando, 1985).
[12] E. Pop *et al.*, Nano Lett. **6**, 96 (2006).
[13] H. B. Casimir and D. Polder, Phys. Rev. **73**, 360 (1948).
[14] J. M. Wylie and J. E. Sipe, Phys. Rev. A **30**, 1185 (1984); **32**, 2030 (1985).
[15] E. A. Hinds and V. Sandoghdar, Phys. Rev. A **43**, 398 (1991).
[16] E. M. Purcell, Phys. Rev. **69**, 681 (1946).
[17] V. V. Klimov, Usp. Fiz. Nauk **46**, 979 (2003).
[18] E. C. Le Ru and P. G. Etchegoin, Chem. Phys. Lett. **423**, 63 (2006).
[19] W. Petrich *et al.*, J. Opt. Soc. Am. B **11**, 1332 (1994); M. Vengalattore, R. S. Conroy, and M. G. Prentiss, Phys. Rev. Lett. **92**, 183001 (2004); H. Chen and E. Riis, Appl. Phys. B **70**, 665 (2000); P. Cren *et al.*, Eur. Phys. J. D **20**, 107 (2002).
[20] S. J. Oldenburg *et al.*, Chem. Phys. Lett. **288**, 243 (1998).
[21] J. M. Obrecht, R. J. Wild, and E. A. Cornell, Phys. Rev. A **75**, 062903 (2007).
[22] C. Monroe *et al.*, Phys. Rev. Lett. **75**, 4011 (1995).
[23] J. Dalibard, J. Dupont-Roc, and C. Cohen-Tannoudji, J. Phys. (Paris) **43**, 1617 (1982).
[24] S. Dimopoulos and A. A. Geraci, Phys. Rev. D **68**, 124021 (2003); D. M. Harber, J. M. Obrecht, J. M. McGuirk, and E. A. Cornell, Phys. Rev. A **72**, 033610 (2005).